Technology and Health Care -1 (2023) 1–18 1
DOI 10.3233/THC-230099
IOS Press

Evaluation of children's oral diagnosis and treatment using imaging examination using AI based Internet of Things

Yan Li[a], Qizhi Qu[b], Yuxue Yue[b], Yuxuan Guo[c,*] and Xiuna Yi[a,*]
[a]*Department of Anesthesiology, Yantai Mountain Hospital, Yantai, Shandong, China*
[b]*CT/MR Division, Liaocheng Third People's Hospital, Liaocheng, Shandong, China*
[c]*Department of Stomatology, Affiliated Hospital of Northwest University/Xi'an Third Hospital, Xi'an, Shaanxi, China*

Received 30 January 2023
Accepted 18 May 2023

Abstract.
BACKGROUND: Although cone beam computed tomography (CBCT) plays an important role in the diagnosis and treatment of oral diseases, its image segmentation method needs to be further improved, and there are still objections about the clinical application effect of general anesthesia (GA) on children's dental fear (CDF).
OBJECTIVE: This study aimed to investigate the application value of CBCT based on intelligent computer segmentation model in oral diagnosis and treatment of children in the context of biomedical signals, and to analyze the alleviating effect of GA on CDF.
METHODS: Based on the regional level set (CV) algorithm, the local binary fitting (LBF) model was introduced to optimize it, and the tooth CBCT image segmentation model CV-LBF was established to compare the segmentation accuracy (SA), maximum symmetric surface distance (MSSD), average symmetric surface distance (ASSD), over segmentation rate (OR), and under segmentation rate (UR) between these models and other algorithms. 82 children with CDF were divided into general anesthesia group (GAG) ($n = 38$) and controls ($n = 44$) according to the voluntary principle of their families. Children in GAG were treated with GA and controls with protective fixed intervention. Children's fear survey schedule-dental subscale (CFSS-DS) and Venham scores were counted before intervention in the two groups. CFSS-DS scores were recorded at 2 hours after intervention and after recovery in children in GAG. CFSS-DS and Venham scores were performed in all children 1 week after surgery.
RESULTS: The results showed that the SA value of CV-LBF algorithm was higher than that of region growing algorithm ($P < 0.05$). OR, UR, MSSD, and ASSD values of CV-LBF algorithm were evidently lower than those of other algorithms ($P < 0.05$). CFSS-DS scores were lower in GAG than in controls 2 hours after intervention and at return visits after 1 week of intervention ($P < 0.001$), and Venham scores were lower in GAG than in controls after intervention ($P < 0.001$). After intervention, the proportion of children with Venham grade 0, 1, 2, and 3 was obviously higher in GAG than in controls ($P < 0.001$), while the proportion of children with Venham grade 4 and 5 was clearly higher in controls than in GAG ($P < 0.001$).
CONCLUSION: The results revealed that the computer intelligent segmentation model CV-LBF has potential application value in CBCT image segmentation of children's teeth, and GA can effectively alleviate anxiety of children with CDF and can be used as biomedical signals.

Keywords: Artificial intelligence, cone beam computed tomography (CBCT), oral cavity in children, general anesthesia, children's dental fear

*Corresponding authors: Yuxuan Guo, Department of Stomatology, Affiliated Hospital of Northwest University/Xi'an Third Hospital, Xi'an, Shaanxi, China. E-mail: queenblade@163.com. Xiuna Yi, Department of Anesthesiology, Yantai Mountain Hospital, Yantai, Shandong, China. E-mail: ytxuxiuzh@126.com.

1. Introduction

As the oral part of the digestive system, teeth play an important role in food chewing and pronunciation [1]. In recent years, with the development of social economy and the improvement of people's health concerns, oral health has attracted more and more attention. According to statistics, the annual number of oral diagnosis and treatment in China is about 300 million, the prevalence of oral diseases is as high as 97.6%, and only 0.22% of the adult population meets the oral health standards [2]. Oral health in children plays an active role in systemic nutritional intake and maxillofacial growth and development, and dental caries is the most common oral disease in children. The oral cavity's development and maintenance, as well as the progression of oral diseases, are influenced by nutrition and diet. These factors play a significant role in the etiology and pathogenesis of oro-facial diseases and disorders. Nutrition and oral health are interdependent, and consuming foods that are rich in calcium and other nutrients such as leafy greens, almonds, cheese, milk, plain yogurt, and calcium-fortified tofu can benefit tooth health. Additionally, protein-rich foods like eggs, milk, poultry, fish, and meat are excellent sources of phosphorus. In trauma theory, protective factors are qualities, situations, or experiences that can help people or communities in protecting off, adjusting with, or recovering from the negative consequences of trauma. They consist of access to resources, resilience, a sense of control, social support, and positive self-image. These factors are important for developing resilience and are frequently the focus of interventions aimed at mitigating the negative effects of trauma. According to statistics, the prevalence of dental caries in children aged 3–5 years in China is as high as 66.0%, and the incidence of dental trauma in children aged 12 years is as high as 19.5% [3], but the visit rate and caries supplementation ratio are only 19.4% and 3.1% [4]. Because the root of the tooth is located in the alveolar bone, in order to accurately understand the tooth arrangement and root distribution and collision characteristics, dentists need to evaluate the tooth status of patients in detail based on imaging techniques, cone beam computed tomography (CBCT) technology can diagnose tooth, periodontal, and jaw diseases due to its advantages of high imaging accuracy and low artifact rate [5]; and in addition, it provides a reference basis for the selection of treatment options and prognosis, so it is used as a common means of diagnosis and treatment of oral diseases. CBCT can not only accurately measure root canal length and volume, root canal curvature, root inclination, but also show the anatomical shape of C-type root canals. In the process of traditional disease diagnosis, CT image segmentation is mainly completed by manual delineation by physicians, which is not only time-consuming, but also has low segmentation efficiency, and has obvious subjectivity [6]. In recent years, with the introduction of computer intelligence technology, CT image segmentation has evolved from traditional threshold algorithms to supervised or unsupervised computer intelligence algorithms [7]. Because there is obvious noise in CBCT images of teeth, the root part belongs to bone structure, which makes alveolar bone and root difficult to distinguish; and the distance between teeth is close, which is easy to produce adhesion on images, and a variety of computer intelligent algorithms can't be directly applied in tooth segmentation. Horizontal set image method avoids the parameterization process of curve tracking and has potential advantages in tooth CT image segmentation [8]. A tooth CT image segmentation model is constructed based on edge level set algorithm. This model has high continuity and smoothness of the segmentation curve, but its segmentation gray distribution is not uniform and needs further optimization [9]. Uneven grey distribution in images can lead to inaccurate and unreliable segmentation, causing over or under-segmentation, sensitivity to lighting, and increased computational requirements.

The current study results suggested that the medical treatment rate of oral diseases in children in China was low, which was related to factors such as weak awareness of oral supervision by parents

and long treatment time of oral diseases. Fear in children was one of the main reasons for low medical treatment rate, and age was inversely proportional to the incidence of anxiety in children [10]. According to statistics, about 48.4%∼83.7% of children aged 3–5 years in oral clinic showed different degrees of children's dental fear (CDF) [11]. CDF refers to the phenomenon that children showed anxiety and fear of psychological state in the diagnosis and treatment of oral diseases, presenting increased sensitivity, reduced tolerance, and even resistance to treatment in behavior. Various methods can be used to measure a child's dental anxiety, including self-report measures, parent report measures, behavioral observation measures, and physiological measures. It's essential to consider the child's age, developmental level, and cultural background, and a combination of methods may be needed for accurate measurement. CDF can be shown through crying, avoidance, physical symptoms, clinging behavior, refusal to cooperate, difficulty sleeping, communication issues, disruptive behavior, and complaints of pain. Early intervention with a pediatric dentist experienced in managing dental fear is crucial. CDF has a serious impact on treatment compliance, odontogenic oral disease development, and maxillofacial (bone) development. In recent years, the incidence of CDF has increased obviously. At present, physiological index assessment method, psychological test method, and behavioral test method are mainly used to evaluate CDF in clinical practice. Among them, physiological index assessment method is cumbersome to operate and difficult to implement in oral diseases. Oral CDF assessment is mainly based on psychological test method, supplemented by behavioral test method. The results of clinical studies have shown that factors such as oral visit environment, pain, child personality, child perception, physical fitness, and parental cognition are common factors in the occurrence of CDF, of which pain is one of the main factors in the occurrence of CDF. Pain during the treatment of oral diseases makes children highly sensitive, the body enters a stress state, finally triggering the occurrence of CDF [12]. The children with oral diseases are prone to develop inferiority complex, which leads to the occurrence of CDF, suggesting that there is an obvious correlation between oral health status and the occurrence of CDF. Psychological, physical, medical immobilization, and drug therapy are adopted to treat CDF in clinical practice [13]. Different intervention methods can be applied to intervene in children with different degrees of anxiety, especially sedation or general anesthesia (GA) for patients with high anxiety [14]. It has been pointed out that GA intervention can reduce the anxiety of patients with dental anxiety [15]. GA intervention can make the diagnosis and treatment of oral diseases go smoothly, it does not fundamentally solve the CDF, but increases the patient's pain sensitivity. Thus, there is still controversy about the clinical effect of GA on CDF [16].

CHI-Net is a medical image segmentation network that utilizes a hierarchical context integration approach to accurately identify important regions in medical images. The network comprises two main modules, DDC and SRF, which work together to achieve superior performance compared to other existing methods for object segmentation in medical images [17]. CANet, a medical image segmentation network that incorporates a dual-stream pyramid module and an encoder-decoder module with context awareness. The network is designed to extract useful information from various medical images by combining these modules. The proposed network aims to improve medical image segmentation accuracy by leveraging the benefits of these different modules [18].

Although CBCT plays an important role in the diagnosis and treatment of oral diseases, its image segmentation method needs to be further improved, and there are still objections about the clinical application effect of GA in CDF. Therefore, based on the level set CT image segmentation method, through improving the algorithm, a tooth CBCT image computer intelligent segmentation model was established, and it was applied to the diagnosis and treatment of dental diseases in children to analyze the performance of the optimization algorithm in CBCT image segmentation. It aimed to investigate the effect of GA in CDF and provide some clinical basis for intelligent diagnosis and treatment of pediatric oral computer and selection of CDF intervention program.

2. Materials and methods

2.1. Study subjects

82 children with CDF who were diagnosed and treated at the Yantai Mountain Hospital from December 2020 to March 2022 were selected as the study subjects. All children underwent CBCT, and the degree of dental anxiety was assessed using the children's fear survey schedule-dental subscale (CFSS-DS) and Venham scale. Inclusion criteria: (1) children aged 3–6 years; (2) children with good general health; (3) children need to return to the dental clinic for many times; (4) CFSS-DS score higher than 34 points, (5) Venham grade $\geqslant 3$; (6) American Society of Anesthesiologists (ASA) physical assessment grade I–II, children without GA contraindications; (7) children without no mental disorders or cognitive impairment; exclusion criteria: (1) ASA grade $\geqslant$ III, GA contraindications; (2) oral diseases complicated by acute inflammation; (3) children with cardiovascular system diseases; (4) children with respiratory diseases; (5) children with mental or mental disorders; (6) children taking anxiolytic and sedative drugs within 7 days before treatment; (7) mild anxiety children whose treatment was not affected; (8) parents refused to participate in this trial; the family members of the children signed informed consent, and the experimental process was approved by the ethics committee of Yantai Mountain Hospital.

2.2. Dental biomedical signal and image preprocessing

CBCT images during oral diagnosis and treatment in Yantai Mountain Hospital were collected and saved as DICOM standard format. All CBCT images were scanned by Italian NEWTOM VGi scanner. The scanning parameters were as follows: tube voltage 110 kV, current 2.81 mA, scanning field of vision 150 mm $\times$ 150 mm, scanning time 6,000 ms, resolution 0.1 mm $\times$ 0.1 mm, axial layer thickness 0.3 mm.

For DICOM biological signal data, image gray value transformation was required. The specific operation method was as follows: window-adding method [19] was adopted to display the gray scale of DICOM format image, and linear mapping between the original gray scale value and the displayed gray scale was established according to the gray scale value of image. It establishes a linear mapping between the original grayscale values and the displayed grayscale. By selecting a specific range of grayscale values, called a window, and mapping it to the full display range, the method enhances the visibility of relevant image details. This allows healthcare professionals to better visualize anatomical structures or pathological features. The implementation of the window-adding method may vary depending on the software or viewer used, and different users may customize the window settings based on their specific requirements. Then, the full gray value of the original image can be expressed as follows.

$$O = \frac{255}{W}\left(V - C + \frac{W}{2}\right) \tag{1}$$

O is the original gray value of the image, V is the displayed gray value of the image, W is the window width, and C is the window level.

The logarithmic transformation method of window function was adopted to map the gray scale of the image, and the gray scale value displayed in the window CBCT image is computed.

$$O(V) = \frac{255\log(V) + 1}{\log(V_{\max})} \tag{2}$$

The CBCT image after gray value transformation needed to be processed by adaptive enhancement algorithm to improve the gray level balance of the image. CLAHE enhancement algorithm was used

to process the image. CLAHE is an image enhancement technique that improves contrast and quality of digital images by dividing them into smaller tiles and applying histogram equalization to each tile individually. Unlike traditional histogram equalization, CLAHE applies the equalization to a limited range of intensity values within each tile and uses a clipping or limiting function to prevent over-enhancement and noise amplification. By combining the enhanced tiles, CLAHE produces an image with improved contrast and quality while avoiding artifacts and noise. The gray value $f(x, y)$ of the processed image is presented as below.

$$f(x,y) = \textit{CLAHE}[h(x-m, y-n), m, n \in W] \tag{3}$$

W is a two-dimensional image template, and m and n are stretching factors.

2.3. Establishment of CBCT image intelligent segmentation model based on level set algorithm

CV model can accurately segment image edges and obtain global convergence, but it still has obvious defects when segmenting images with uneven gray distribution. However, they have significant limitations for images with an uneven gray distribution. Such images present difficulties for CV models, resulting in errors such as inaccurate edge detection, boundary placement, and sensitivity to local variations. The segmentation performance of these models is being actively enhanced by researchers in order to better handle uneven gray distribution and improve segmentation accuracy [20]. For the CBCT image after adaptive enhancement processing, if CV is used for processing, its level set energy function $E(\theta)$ is computed.

$$E(\theta) = \gamma E_g(\theta) + \tau E_l(\theta) \tag{4}$$

E_g is the global driving energy function, E_l is the local driving energy function, γ is the global driving energy function parameter, and τ is the local driving energy function parameter.

Based on global information, E_g can increase the image contour and robustness of noise.

$$E_g = \alpha_1 \int Q_1 |I_i(x) - B_1|^2 H_\beta[\theta(x)] dx + \alpha_2 \int Q_1 |I_i(x) - B_2|^2 \{1 - H_\beta[\theta(x)]\} dx \tag{5}$$

B_1 is the average gray level in the evolution curve, B_2 is the average gray level outside the evolution curve, $H_\beta[\theta(x)]$ is a regularized Heaviside function.

Local binary fitting (LBF) model can solve the problem of image segmentation accuracy with uneven gray scale, but it is highly dependent on the initial contour position [21]. LBF model is introduced into the local driving energy function of CV model to avoid the shortcomings of CV model in segmenting images with uneven gray distribution. The accuracy of the Local Binary Fitting (LBF) model for image segmentation in the presence of uneven grayscale depends greatly on the initial contour position. The model iteratively refines the contour based on local image information and prior knowledge of the object shape. Howeve an incorrect initial contour placement can lead to inaccurate segmentation. Therefore, selecting the optimal initial contour position is crucial to achieve precise segmentation results.

$$E_l = \alpha_3 \int Q_1 |I_i(x) - B_1|^2 dx + \alpha_4 \int Q_1 \frac{1}{2} |I_i(x) - B_2|^2 H_\beta[\theta(x)] dx \tag{6}$$

The regularization term is introduced in Eq. (6) to constrain the shape change of root canal segmentation contour, so the level set energy functions are expressed as follows.

$$E(\theta) = \gamma E_g(\theta) + \tau E_l(\theta) + \varepsilon E_r(\theta) \tag{7}$$

$$E_r(\theta) = \mu L(\theta) + \sigma P(\theta) \tag{8}$$

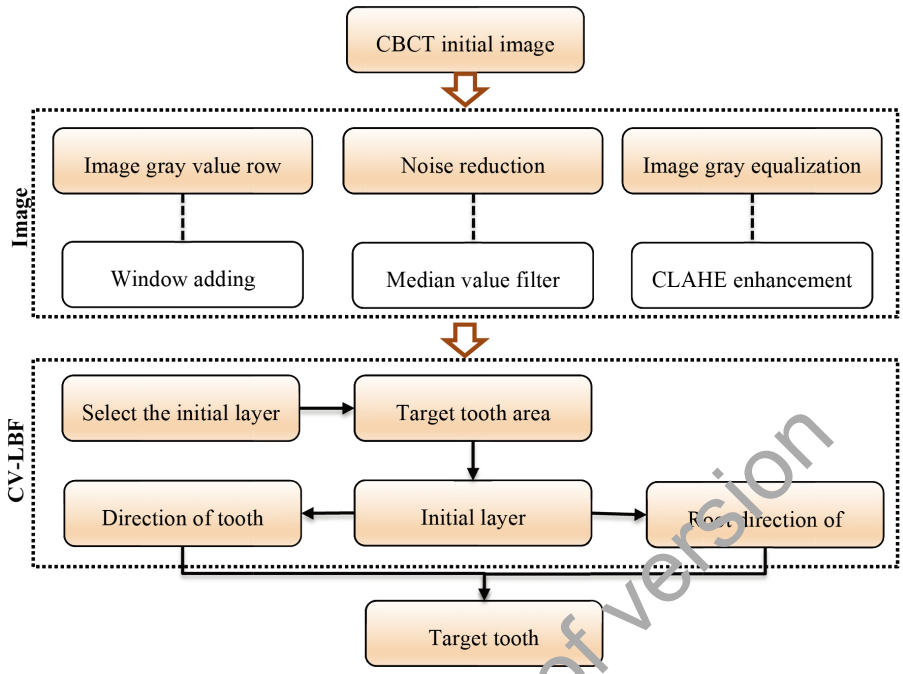

Fig. 1. Flowchart of CBCT images of teeth segmented by CV-LBF model.

$$L(\theta) = \int Q\delta_\beta(x)[|\theta(x)|]dx \tag{9}$$

$$P(\theta) = \frac{1}{2}\int Q[|\theta(x)| - 1]^2 dx \tag{10}$$

$L(\theta)$ is the length penalty item; $P(\theta)$ is the energy penalty term, $E_r(\theta)$ is a regularized item, μ is control parameter for the length penalty item, σ is control parameters for energy penalty item.

The specific process of CV-LBF model segmentation of tooth CBCT image is shown in Fig. 1.

First, the windowing method is applied to transform the image gray value, the median filter is used to denoise the image, and the CLAHE enhancement algorithm to improve the gray balance of CBCT image. The median filter reduces noise in images by replacing each pixel with the median value of its neighboring pixels, making it effective at removing isolated noisy pixels without affecting the image details and edges. Its adaptability to the local image structure, rather than a fixed kernel size, helps preserve the image quality. An appropriate initial layer image is selected to obtain a small window area containing the target teeth. The level set segmentation method is adopted to perform the initial layer results. In children's oral diagnosis and treatment, level set segmentation is utilized to segment the oral cavity and teeth from other structures in the image. This involves image acquisition, preprocessing, initialization, evolution, and postprocessing to extract a final contour for diagnosis and treatment planning. The resulting segmented image can be analyzed to detect abnormalities and plan orthodontic treatments or oral surgeries. Based on the initial layer segmentation, the CV-LBF tooth segmentation model in the direction of the crown and root respectively for fine segmentation, the target tooth segmentation image is obtained.

2.4. CBCT image evaluation index

The performance of CBCT images was evaluated with segmentation accuracy (SA), maximum symmetrical surface distance (MSSD), average symmetrical surface distance (ASSD), over segmentation rate

(OR), and under segmentation rate (UR). Maximum Symmetrical Surface Distance (MSSD) and Average Symmetric Surface Distance (ASSD) are two metrics that assess the precision of image registration algorithms by measuring the distance between two surfaces in a symmetric manner. They share the feature of being used in medical imaging to align images of the same patient taken at different times or align images from different patients to a common coordinate system. However, the main contrast between them is that while MSSD computes the maximum distance between the two surfaces, ASSD measures the average distance. The segmentation result of optimized CV-LBF algorithm was compared with those of adaptive threshold [22], region growing [23], DRLSE [24] and CV algorithms [25]. Adaptive thresholding is an image processing technique that adjusts the threshold for each pixel or region based on local image properties, useful for enhancing visibility and segmenting regions of interest in CBCT images. Region growing is a segmentation algorithm that groups neighboring pixels or voxels based on similarity, allowing for the extraction of distinct regions in CBCT images. Distance Regularized Level Set Evolution (DRLSE) is a level set-based segmentation algorithm that accurately captures complex shapes and boundaries of anatomical structures in CBCT images and finally computer vision algorithms encompass various techniques used for tasks such as image registration, feature extraction, object detection, and classification in CBCT image evaluation, enabling tasks like image alignment, quantitative analysis, and automated quality control.

$$SA = \left[1 - \frac{|R - T|}{R}\right] \times 100\% \tag{11}$$

$$OR = \frac{S}{R} \times 100\% \tag{12}$$

$$UR = \frac{U}{R} \times 100\% \tag{13}$$

R is the tooth or root canal area of the physician manually segmented image; T is the area of the intelligent segmented image, S is the area of the intelligent segmented image extended outside the R contour, and U is the area of the intelligent segmented image contracted into the R contour. When OR and $RU < 10\%$ or $SA > 80\%$, it is considered that the tooth image segmentation is qualified, and the smaller the MSSD and ASSD values, the closer the computer results are to the manual results, and the better the segmentation results are.

2.5. Intervention modalities in children with CDF

According to the voluntary principle, the family members of cldren with CDF chose the intervention method, of which 38 children were in the general anesthesia group (GAG) and the remaining 44 children chose the protective fixation intervention method and they were in controls. Before treatment, the two groups of children through the cartoons, toys, doctors dress, and other means to establish a warm and relaxed treatment environment, preoperative nurses through chatting with children and other means to promote a sense of trust, making the children's mood relaxed.

The child in controls was fasted and water deprived for more than 4 hours before surgery, and the family signed the informed consent form for protective fixation therapy. The nurse assisted the child to lie supine on the oral treatment chair and adjust it to the appropriate height, and the restraint plate was placed flat on the oral treatment chair to fix the top of the restraint plate and the headrest. The child was wrapped with a restraint plate towel to expose only the child's head and neck. During oral treatment, the family assisted with head immobilization and mouthpiece was used to assist the child's mouth opening.

Children in GAG were fasted and water deprived for 8 hours before anesthesia. All children underwent GA using intravenous inhalation combined anesthesia technique. Combining inhalation anesthetics is common in anesthesia practice because it allows for a more precise and reliable level of anesthesia while reducing the risk of side effects associated with higher concentrations of a single agent. This approach also enables synergistic effects and reduced side effects, as well as flexibility in tailoring the anesthetic to the individual patient and procedure. After entering the operating room, the child underwent sedation, arteriovenous puncture, GA, and other operations. The assistant recorded the intraoperative conditions in detail. At the end of the operation, the patient was transferred to the GA recovery room and could leave the hospital after the vital signs were stable for 2 hours.

2.6. Outcome measures

CFSS-DS and Venham [26] scores were counted before intervention in both groups, and CFSS-DS scores were also recorded at 2 hours after intervention in controls, after recovery in GAG. CFSS-DS and Venham scores were performed in all children at return visit 1 week after surgery.

The CFSS-DS [27] was rated 1 to 5 points according to the degree of fear, 5 points for very fear, 4 for more fear, 3 for comparative fear, 2 for a little fear, and 1 for no fear, with a total of 17 items, and with a total score of more than 42 indicating a high level of fear and less than 42 indicating a low level of fear.

2.7. Statistical methods

Data were statistically analyzed using SPSS 22.0. The included measurement data were in accordance with the normal distribution, the measurement data were presented as mean $\pm$ standard deviation ($\bar{x} \pm s$), and the variables between groups were compared adopting the independent sample t-test; percentage (%) indicated the enumeration data, and the chi-square test was applied. Statistical significance was defined as $P < 0.05$.

3. Results

3.1. CBCT image segmentation results for CV-LBF model teeth

The CV-LBF model segments root canals in CBCT images by extracting local binary features and training a machine learning algorithm to predict root canal boundaries. It is trained on annotated datasets and can be used to segment the root canals of individual or multiple teeth, as well as images taken at different angles. CV-LBF model was applied to segment the root canals of teeth at different positions in CBCT images, and the results are illustrated in Fig. 2. CV-LBF model can accurately segment the root canals of teeth with different morphologies.

The CV-LBF model (red) was compared with the manual segmentation (green) (Fig. 3), and the tooth segmentation contours of the CV-LBF model were highly coincident with the manual segmentation results.

3.2. Comparison of tooth segmentation accuracy of intelligent algorithm

The performance of various image segmentation algorithms on CBCT images, measured using the

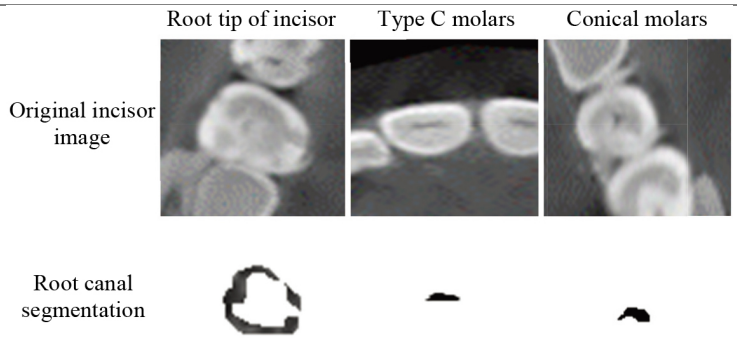

Fig. 2. Automatic segmentation diagram of root canal of CV-LBF model.

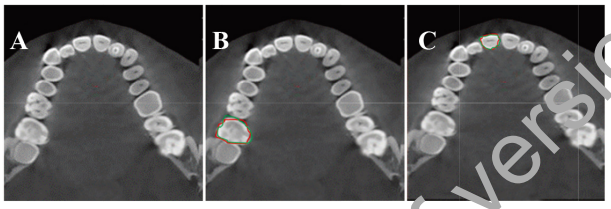

Fig. 3. CBCT cross-sectional tooth segmentation results. A: original CBCT image; B: molar segmentation result; C: incisor segmentation result.

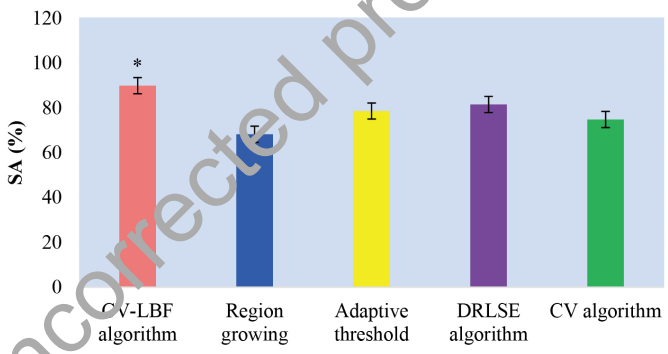

Fig. 4. Comparison of SA values of CBCT images of teeth segmented by different algorithms. * indicates statistical difference compared with region growing algorithm, $P < 0.05$.

SA (segmentation accuracy) value. The algorithms evaluated were CV-LBF, adaptive threshold, region growing, DRLSE, and CV. The results show that the CV-LBF algorithm achieved the highest SA value of (89.92 ± 8.25) %, followed by DRLSE (68.20 ± 6.94) %, region growing (78.63 ± 7.71) %, CV (81.52 ± 6.98) %, and adaptive threshold algorithms (74.86 ± 6.77) %. Among these, the difference in the SA values of the CV-LBF and region growing algorithms was statistically significant ($P < 0.05$), indicating that the former performed better than the latter (Fig. 4).

The OR value is a common metric used to evaluate the similarity between the segmented object and the ground truth object. It represents the ratio of the intersection between the segmented object and the ground truth object to the union of the two objects. A higher OR value indicates a better segmentation accuracy. The results find that the OR values of tooth CBCT images segmented by the CV-LBF (1.53 ± 0.11) %, region growing (5.56 ± 0.34) %, adaptive threshold (3.27 ± 0.26) %, DRLSE (1.84 ± 0.15)

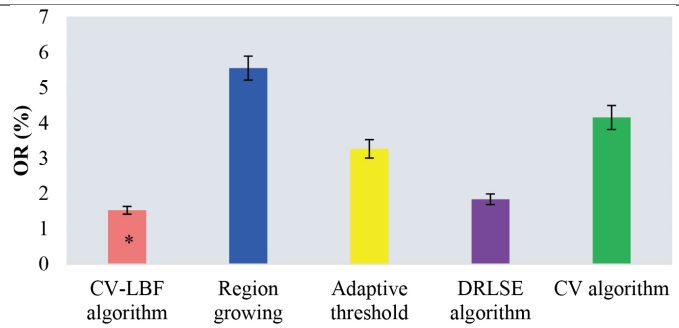

Fig. 5. Comparison of OR values of CBCT images of teeth segmented by different algorithms.

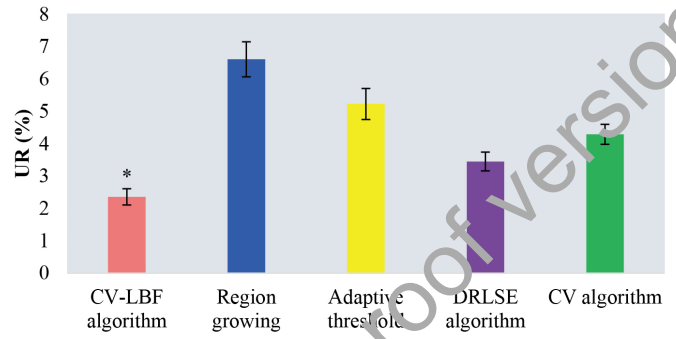

Fig. 6. Comparison of UR values of segmenting CBCT images by different algorithms.

%, and CV (4.16 ± 0.34) % algorithms were lower compared to the OR values of tooth CBCT images segmented by the region growing and CV algorithms. Specifically, the OR value of the CV-LBF algorithm was significantly lower than the OR value of the region growing algorithm ($P < 0.05$), which indicates that the CV-LBF algorithm outperformed the region growing algorithm in terms of segmentation accuracy (Fig. 5).

UR is a metric used to assess the accuracy of a segmentation algorithm, which calculates the ratio of the union of the ground truth and segmented regions to their intersection. It indicates how much of the true positive region is correctly segmented by the algorithm. CV-LBF (2.36 ± 0.25) %, Region growing (6.61 ± 0.54) %, Adaptive threshold (5.23 ± 0.48) %, DRLSE (3.45 ± 0.29) %, and CV (4.29 ± 0.31) %. The CV-LBF algorithm showed a significantly lower mean UR value compared to the region growing algorithm ($p < 0.05$), indicating better performance in accurately segmenting dental CBCT images (Fig. 6).

3.3. Comparison of MSSD and ASSD values of CBCT image segmentation with intelligent algorithm

The evaluation metric used to compare the algorithms was the Mean Symmetric Surface Distance (MSSD), which measures the average distance between corresponding points on the surfaces of the segmented image and the ground truth image. The CV-LBF, region growing, adaptive threshold, DRLSE, and CV algorithms were compared, in which the MSSD values obtained for each algorithm were (1.98 ± 0.71), (9.35 ± 0.96), (7.39 ± 0.78), (10.26 ± 3.03), and (12.97 ± 2.15) mm, respectively. From the results, it is clear that the CV-LBF algorithm performed better than the CV algorithm, as the MSSD value obtained for CV-LBF was significantly lower ($P < 0.05$) than that CV (Fig. 7).

Table 1
Basic data of patients

Factor	GAG ($n = 38$)	Controls ($n = 44$)	χ^2/t	P
Gender [case (%)]			0.796	0.315
Male	18 (47.37%)	21 (47.73%)		
Female	20 (52.63%)	23 (52.27%)		
Age (years)	4.53 ± 1.29	4.39 ± 2.01	0.223	0.734
Parenting style			0.583	0.401
Parenting rearing	30 (78.95%)	33 (75.00%)		
Grandparental rearing	8 (21.05%)	11 (25.00%)		
Only child			1.753	0.226
Yes	23 (60.53%)	28 (63.64%)		
No	15 (39.47%)	16 (36.36%)		
Mode of delivery			0.441	0.503
Spontaneous delivery	26 (68.42%)	29 (65.91%)		
Caesarean section	12 (31.58%)	15 (34.09%)		

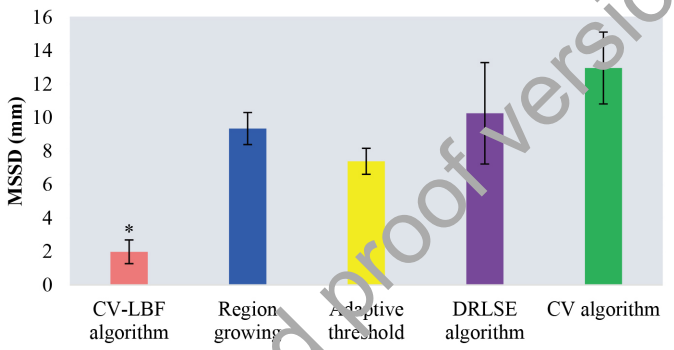

Fig. 7. Comparison of MSSD values of segmenting CBCT images by different algorithms. *Indicates statistical difference compared with CV algorithm, $P < 0.05$.

ASSD is a widely used metric that measures the distance between the surfaces of two segmented objects. The CV-LBF, regional growth, adaptive threshold, DRLSE, and CV are the five different algorithms tested in the experiment. The average ASSD values obtained for each algorithm were (0.27 ± 0.03), (6.64 ± 0.58), (2.05 ± 0.33), (5.16 ± 0.25), and (5.02 ± 0.48) mm, respectively. The CV-LBF algorithm performed better than the regional growth algorithm, as the ASSD value obtained for CV-LBF was significantly lower ($P < 0.05$). The CV-LBF algorithm was more accurate in segmenting the CBCT images and produced segmentations that were closer to the ground truth image (Fig. 8).

3.4. Comparison of clinical characteristics of children with CDF before intervention

Statistical analysis was performed on the age, gender, parenting style, whether the child was the only child, and mode of delivery of GAG and controls (Table 1). The results indicated that there were no statistically significant differences in the age, gender, parenting style, whether the child was the only child, and mode of delivery between two groups ($P > 0.05$).

3.5. Comparison of education level of mothers and family income

There were not clear different in maternal education level and family income between the two groups ($P > 0.05$) (Fig. 8).

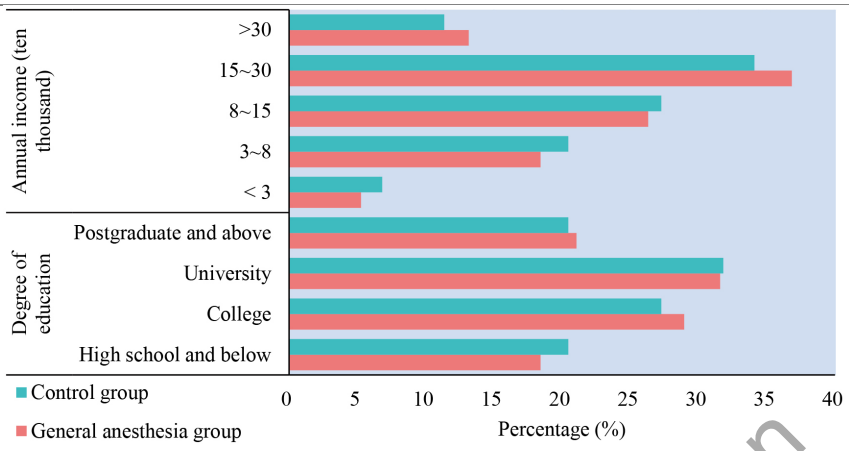

Fig. 8. Comparison of family income and maternal education level.

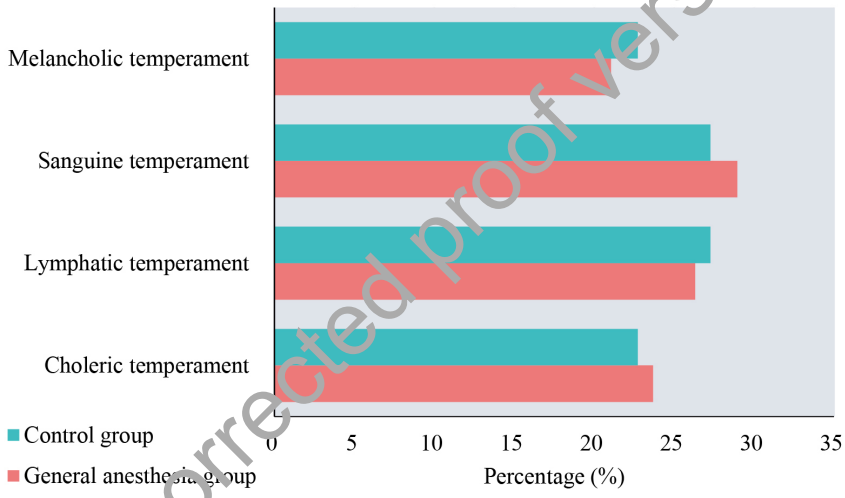

Fig. 9. Comparison of temperament type distribution.

3.6. Comparison of distribution of temperament types in children

Figure 9 shows the proportion of different temperament types in the two groups, 9 (23.68%), 10 (26.32%), 11 (28.95%), and 8 (21.05%) children with phlegmatic temperament, biliary temperament, sanguine temperament, and depressive temperament in GAG; 10 (22.73%), 12 (27.27%), 12 (27.27%), and 10 (22.73%) children in controls, respectively ($P > 0.05$).

3.7. Comparison of CFSS-DS values at different time periods before and after intervention

Before intervention, the CFSS-DS scores of GAG and controls were (35.47 ± 2.97) and (35.26 ± 3.13) ($P > 0.05$). The CFSS-DS scores of GAG and controls after 2 hours of intervention were (26.71 ± 2.22) and (38.55 ± 3.46). After 2 hours of intervention, relative to before intervention, the score of GAG was (8.76 ± 5.72) lower, and the score of GAG was (3.29 ± 2.76) higher. After 2 hours of intervention, the

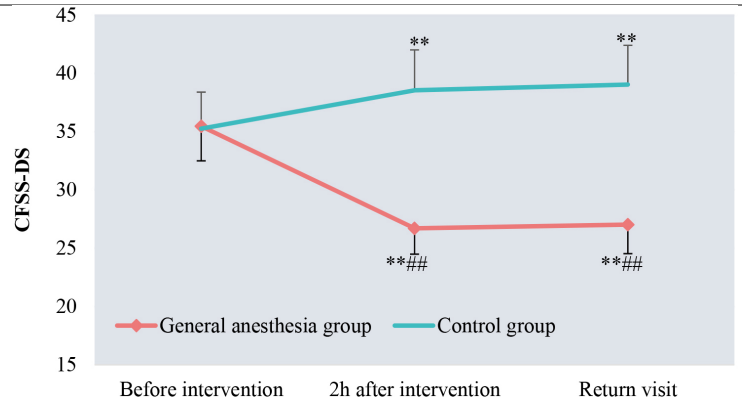

Fig. 10. Comparison of CFSS-DS values at different time periods before and after intervention. ** Means compared with before intervention, $P < 0.001$; ## means compared with controls, $P < 0.001$.

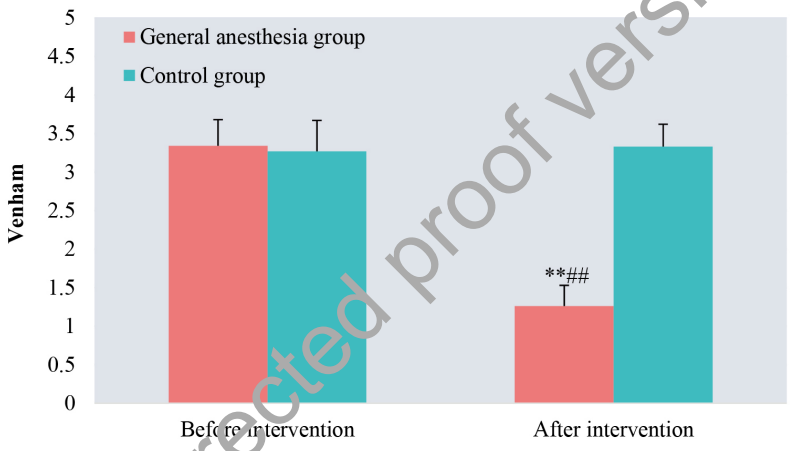

Fig. 11. Comparison of Venham scores before and after intervention.

score of GAG was lower ($P < 0.001$), the score of controls was higher ($P < 0.001$), and the score of GAG after 2 hours of intervention was lower relative to controls ($P < 0.001$). The score of GAG and controls at return visit after 1 week of intervention were (27.03 ± 2.49) and (39.04 ± 3.37). At return visit after 1 week of intervention, compared with before intervention, the score of GAG was (8.44 ± 6.26) lower, and that of controls was (3.78 ± 3.11) higher; the score of GAG was obviously lower ($P < 0.001$), and that of controls was higher ($P < 0.001$); the score of GAG at return visit after 1 week of intervention was lower in contrast with controls ($P < 0.001$). There was no significant difference in CFSS-DS score at return visits after 1 week of intervention compared with that after 2 hours of intervention between the two groups ($P > 0.05$) (Fig. 10).

3.8. Comparison of Venham scores before and after intervention

There was not obviously different in Venham scores between the two groups before intervention ($P > 0.05$), Venham scores after intervention were (1.26 ± 0.27) and (3.33 ± 0.29), and after intervention, the score of GAG decreased ($P < 0.001$), and was lower than that of controls ($P < 0.001$). In controls,

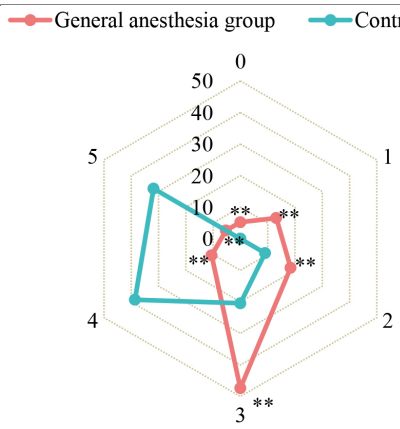

Fig. 12. Comparison of Venham grade distribution after intervention. **Means $P < 0.001$ relative to controls.

Venham score before the intervention was not clearly different from that after the intervention ($P > 0.05$) (Fig. 11).

Before the intervention, GAG had 14 (36.84%), 13 (34.21%), and 11 (28.95%) children with Venham grade 3, 4, and 5, 16 (36.36%), and controls had 16 (36.36%), 17 (38.64%), and 11 (25.00%) children ($P > 0.05$). After intervention, the proportion of children with grade 0, 1, 2 and 3 was higher in GAG than in controls ($P < 0.001$), while the proportion of children with grade 4 and 5 was higher in controls than in GAG ($P < 0.001$) (Fig. 12).

4. Discussion

It was found that relative to regional growth algorithm, the value of CV-LBF algorithm was higher, the OR and UR values were lower ($P < 0.05$), and the MSSD and ASSD values of CV-LBF algorithm were lower than those of other algorithms, suggesting that the established model CV-LBF has a better segmentation effect on dental CBCT images. The reason may be because the CV-LBF model increases the curve evolution and convergence performance of the model and constrains the shape change of root canal segmentation contour, so its segmentation accuracy increases obviously. It has been pointed out that during root canal segmentation of a single tooth, the LBF (Local Binary Fitting) algorithm accurately assesses neighboring teeth by comparing the similarity of their root canal contour curves. This algorithm analyzes dental imaging data, extracts the root canal contours, and applies a binary fitting method to compare factors like shape, size, and spatial relationships. By evaluating the degree of similarity, the LBF algorithm helps make precise judgments about dental conditions and treatment approaches, aiding in restoration planning and improving overall dental care quality [28]. The DRLSE (Distance Regularized Level Set Evolution) model algorithm is effective at segmenting root fuzzy edges, but it may struggle to accurately segment the vanishing edge of the crown. The algorithm's difficulty with the vanishing edge can be attributed to lower edge contrast, complex background elements, and variations in lighting conditions. To improve segmentation in these cases, additional techniques or modifications to the algorithm may be needed, such as incorporating advanced edge detection methods or considering object-level context [29].

C-type roots in molar root canals have irregular shapes, making them challenging to accurately segment during intelligent imaging. In China, approximately 32% of root canals are classified as C-type. The

irregularities of these canals pose difficulties in identifying their boundaries and associated structures, leading to potential treatment complications. Dental professionals need to be well-prepared to address these challenges by utilizing advanced techniques and staying updated with the latest advancements in endodontics [30,31]. The results suggested that the CV-LBF model could accurately segment the root canals of teeth with different morphologies, and the segmentation results were highly coincident with the manual delineation contours, showing that the CV-LBF model has potential application value in the segmentation of dental CBCT images.

The results of the current study revealed that parental education level, family economic income, and personality type of children with oral diseases will have a certain impact on CDF [32]. The above factors in GAG and controls were statistically analyzed. There was no statistical difference in maternal education level, family income, and personality type of children between the two groups ($P > 0.05$), suggesting that the intervention measures were comparable. Although a variety of interventions are currently used in the treatment of children with CDF, there are no clear and effective interventions. Children's dental fear (CDF) is addressed using a range of methods, including behavior modification techniques, cognitive behavioral therapy (CBT), medicinal treatments, virtual reality therapy, involvement of parents, and desensitization. The sort of intervention utilized will depend on the degree of the fear and the child's requirements. Collaboration between the children, parents, and the dentist is essential for optimal treatment results. GA was used to intervene children with CDF, and the results showed that the CFSS-DS scores of GAG were lower after 2 hours of intervention and at return visits after 1 week of intervention ($P < 0.001$). Protective fixed intervention increases anxiety in relieving oral diagnosis and treatment in children and GA relieves oral diagnosis and treatment anxiety in children with CDF. GA can be applied to the oral diagnosis and treatment of CDF in children with extreme anxiety and has a positive effect on the oral health of children. Genetic algorithms applied to the diagnosis and treatment of dental caries in anxious children improves oral health outcomes. GA optimizes diagnosis, customizes treatment plans, and reduces factors that cause anxiety. This strategy inspires regular dental visits, early detection, and prompt treatment, resulting in improved oral health over the long term. Integrating general anesthesia with comprehensive care is essential for effectively treating anxiety [33]. In addition, some studies have presented that GA intervention will not damage the patient's brain, no pain during surgery, memory temporarily disappears, and the incidence of psychological problems such as postoperative depression and fear is low, which is worthy of application in the diagnosis and treatment of oral diseases. To assess the frequency of emergence agitation in pediatric patients undergoing general anesthesia by investigating the effects of midazolam administration in the operating room and postoperative recovery area. The patients were separated into three groups, receiving either midazolam or saline 30 minutes prior to the completion of dental treatment [34]. However, the GA can't fundamentally solve CDF and even aggravate CDF symptoms in children, resulting in worse oral health status in children intervened by GA [35]. Protective fixation, as a traditional intervention in stomatology, has been widely applied in oral diagnosis and treatment of preschool children, and some studies have revealed that the use of protective fixation measures can improve children's treatment compliance [36]. The results indicated that protective fixation measures could not alleviate anxiety in children with CDF. Ichikawa et al. [37] pointed out that protective fixation measures would bring psychological trauma and adverse emotions to children, which mirrors our results.

5. Conclusion

A tooth CBCT image segmentation optimization algorithm CV-LBF was established to investigate its

application value in the segmentation of tooth CBCT images in children. The effect of GA on anxiety relief in CDF was investigated in children with CDF. It is found that the intelligent model CV-LBF has high accuracy in segmenting tooth CBCT images and has potential application value, and GA intervention can effectively alleviate CDF anxiety. However, there are still some shortcomings, the compliance of children at return visit after intervention is not analyzed, and the effect of GA intervention on the compliance of children with CDF will be further analyzed in future work to provide more comprehensive data support for its application in pediatric stomatology. In conclusion, it provides some clinical basis for pediatric oral computer intelligent diagnosis and treatment and selection of CDF intervention program.

Funding

The authors did not receive any funding.

Conflict of interest

The authors do not have any conflicts of interest to report.

Data availability statement

No datasets were generated or analyzed during the current study.

Author contributions

All authors contributed to the design and methodology of the study, assessment of the outcomes and writing of the manuscript.

References

[1] Xiao J, Fiscella KA, Gill SR. Oral microbiome: Possible harbinger for children's health. Int J Oral Sci. 2020; 12(1): 12.
[2] Kazeminia M, Abdi A, Shohaimi S, Jalali R, Vaisi-Raygani A, Salari N, Mohammadi M. Dental caries in primary and permanent teeth in children's worldwide, 1995 to 2019: A systematic review and meta-analysis. Head Face Med. 2020; 16(1): 22.
[3] Wang Z B, Ma Y, Liu H, et al. Simultaneous determination and pharmacokinetics of tetrandrine, fangchinoline, and cyclanoline in rat plasma by ultra-high performance liquid chromatography-mass spectrometry after oral administration of stephaniae tetrandrae radix extract. World Journal of Traditional Chinese Medicine, 2021; 7(1): 130.
[4] Keels MA. Personalized dental caries management in children. Dent Clin North Am. 2019; 63(4): 621-629.
[5] Alsadat FA, Alamoudi NM, El-Housseiny AA, Felemban OM, Dardeer FM, Saadah OI. Oral and dental manifestations of celiac disease in children: A case-control study. BMC Oral Health. 2021; 21(1): 669.
[6] Wan ZB, Dong YQ, Yu ZC, Lv HB, Lv ZH. Semi-Supervised Support Vector Machine for Digital Twins Based Brain Image Fusion. 2021; 15: 802.
[7] Zhou X, Li Y, Liang W. CNN-RNN based intelligent recommendation for online medical pre-diagnosis support. IEEE/ACM Transactions on Computational Biology and Bioinformatics, 2021; 18(3): 912-921.
[8] Cakir Karabas H, Ozcan I, Erturk AF, Guray B, Unsal G, Senel SN. Cone-beam computed tomography evaluation of impacted and transmigrated mandibular canines: A retrospective study. Oral Radiol. 2021 Jul; 37(3): 403-411.

[9] Mizuhashi F, Ogura I, Sugawara Y, Oohashi M, Mizuhashi R, Saegusa H. Diagnosis of root fractures using cone-beam computed tomography: Difference of vertical and horizontal root fracture. Oral Radiol. 2021; 37(2): 305-310.
[10] Dias FMCS, Gradella CMF, Ferreira MC, Oliveira LB. Molar-incisor hypomineralization: Parent's and children's impact perceptions on the oral health-related quality of life. Eur Arch Paediatr Dent. 2021 Apr; 22(2): 273-282.
[11] Alsadat FA, El-Housseiny AA, Alamoudi NM, Elderwi DA, Ainosa AM, Dardeer FM. Dental fear in primary school children and its relation to dental caries. Niger J Clin Pract. 2018; 21(11): 1454-1460.
[12] Wu L, Gao X. Children's dental fear and anxiety: Exploring family related factors. BMC Oral Health. 2018; 18(1): 100.
[13] Panda S, Quadri MFA, Hadi IH, Jably RM, Hamzi AM, Jafer MA. Does dental fear in children predict untreated dental caries? An analytical cross-sectional study. Children (Basel). 2021 May 12; 8(5): 382.
[14] Yon MJY, Chen KJ, Gao SS, Duangthip D, Lo ECM, Chu CH. An introduction to assessing dental fear and anxiety in children. Healthcare (Basel). 2020; 8(2): 86.
[15] Guney SE, Araz C, Tirali RE, Cehreli SB. Dental anxiety and oral health-related quality of life in children following dental rehabilitation under general anesthesia or intravenous sedation: A prospective cross-sectional study. Niger J Clin Pract. 2018 Oct; 21(10): 1304-1310.
[16] Galeotti A, Garret Bernardin A, D'Antò V, Ferrazzano GF, Gentile T, Viarani V, Cassabgi G, Cantile T. Inhalation conscious sedation with nitrous oxide and oxygen as alternative to general anesthesia in uncooperative, fearful, and disabled pediatric dental patients: A large survey on 688 working sessions. Biomed Res Int. 2016; 2016: 7289310.
[17] Xie X, Pan X, Zhang W, An J. A context hierarchical integrated network for medical image segmentation. Computers and Electrical Engineering. 2022; 101: 108029.
[18] Xie X, Zhang W, Pan X, Xie L, Shao F, Zhao W, An J. CANet: Context aware network with dual-stream pyramid for medical image segmentation. Biomedical Signal Processing and Control. 2023; 81: 104437.
[19] Xu L, Zhang XD, Zeng C, Yang HF. Analysis of missed diagnosis of gastric lipomas by CT. Curr Med Imaging. 2021; 17(7): 911-915.
[20] Satpute N, Gómez-Luna J, Olivares J. Accelerating Chan-Vese model with cross-modality guided contrast enhancement for liver segmentation. Comput Biol Med. 2020; 124: 103930.
[21] Haghnegahdar AA, Kolahi S, Khojastepour L, Tajeripour F. Diagnosis of tempromandibular disorders using local binary patterns. J Biomed Phys Eng. 2018; 8(1): 87-96.
[22] Sun H, Yang J, Fan R, Xie K, Wang C, Ni X. Stepwise local searching ultrasound image algorithms based on adaptive iterative threshold Harris corner features. Medicine (Baltimore). 2020; 99(37): e22189.
[23] Jiang Y, Qian J, Lu S, Tao Y, Lin J, Lin H. LRVRG: A local region-based variational region growing algorithm for fast mandible segmentation from CBCT images. Oral Radiol. 2021; 37(4): 631-640.
[24] Zheng J, Zhang D, Huang K, Sun Y. A CBCT series slice image segmentation method. J Xray Sci Technol. 2018; 26(5): 815-832.
[25] Nag MK, Chatterjee S, Sadhu AK, Chatterjee J, Ghosh N. Computer-assisted delineation of hematoma from CT volume using autoencoder and Chan Vese model. Int J Comput Assist Radiol Surg. 2019; 14(2): 259-269.
[26] Rath S, Das D, Sahoo SK, Raj A, Gudha NR, Rathee G. Childhood dental fear in children aged 7–11 years old by using the Children's Fear Survey Schedule-Dental Subscale. J Med Life. 2021 Jan-Mar; 14(1): 45-49.
[27] Dahlander A, Soares F, Grindefjord M, Dahllöf G. Factors associated with dental fear and anxiety in children aged 7 to 9 years. Dent J (Basel). 2019; 7(3): 68.
[28] Zou Y, Yao G, Wang J. Research on 3D crack segmentation of CT images of oil rock core. PLoS One. 2021 Oct 14; 16(10): e0258463.
[29] Zhang L, Zhao J, Yang L, Jiang Z, Li Q. Unsupervised scoliosis diagnosis via a joint recognition method with multifeature descriptors and centroids extraction. Comput Math Methods Med. 2018; 2018: 6213264.
[30] Brea G, Gomez F, Gomez-Sosa JF. Cone-beam computed tomography evaluation of C-shaped root and canal morphology of mandibular premolars. BMC Oral Health. 2021; 21(1): 236.
[31] Ren HY, Zhao YS, Yoo YJ, Zhang XW, Fang H, Wang F, Perinpanayagam H, Kum KY, Gu Y. Mandibular molar C-shaped root canals in 5th millennium BC China. Arch Oral Biol. 2020 Sep; 117: 104773.
[32] Ghaderi F, Solhjou N. The effects of lavender aromatherapy on stress and pain perception in children during dental treatment: A randomized clinical trial. Complement Ther Clin Pract. 2020; 40: 101182.
[33] López-Velasco A, Puche-Torres M, Carrera-Hueso FJ, Silvestre FJ. General anesthesia for oral and dental care in paediatric patients with special needs: A systematic review. J Clin Exp Dent. 2021 Mar 1; 13(3): e303-e312.
[34] Kawai M, Kurata S, Sanuki T, Mishima G, Kiriishi K, Watanabe T, Ozaki-Honda Y, Yoshida M, Okayasu I, Ayuse T, Tanoue N, Ayuse T. The effect of midazolam administration for the prevention of emergence agitation in pediatric patients with extreme fear and non-cooperation undergoing dental treatment under sevoflurane anesthesia, a double-blind, randomized study. Drug Des Devel Ther. 2019; 13: 1729-1737.
[35] Ohtawa Y, Yoshida M, Fukuda K. Parental satisfaction with ambulatory anesthesia during dental treatment for disabled individuals and their preference for same in future. Bull Tokyo Dent Coll. 2019; 60(1): 53-60.

[36] Singh S, Neyaz N, Tanwar AS, Patil AN, Khan AM, Kakti A. Propofol's efficacy and outcomes on anxious children's behavior in the course of dental therapy: An interventional trial. J Pharm Bioallied Sci. 2022; 14(Suppl 1): S550-S553.
[37] Ichikawa K, Fujiwara T, Kawachi I. Prenatal alcohol exposure and child psychosocial behavior: A sibling fixed-effects analysis. Front Psychiatry. 2018; 9: 570.